Enhanced Molecular Diffusivity Through Destructive Interference Between Electrostatic and Osmotic Forces

Journal:	*The Journal of Physical Chemistry Letters*
Manuscript ID	jz-2021-01875n.R1
Manuscript Type:	Letter
Date Submitted by the Author:	n/a
Complete List of Authors:	Samanta, Tuhin; Arizona State University, Physics Mostajabi Sarhangi, Setare; Arizona State University, School of Molecular Sciences and Department of Physics Matyushov, Dmitry; Arizona State University, School of Molecular Sciences and Department of Physics

Enhanced Molecular Diffusivity Through Destructive Interference Between Electrostatic and Osmotic Forces

Tuhin Samanta, Setare Mostajabi Sarhangi, and Dmitry V. Matyushov*

School of Molecular Sciences and Department of Physics, Arizona State University, PO Box 871504, Tempe, AZ 85287-1504

E-mail: dmitrym@asu.edu, Tel:(480)965-0057

Abstract

Molecular charge asymmetrically distributed in a diffusing tagged particle causes a nonzero electrostatic force balanced by an opposing van der Waals (vdW) force. Fluctuations of electrostatic and vdW forces are highly correlated, and they destructively interfere in the force variance. This phenomenology is caused by the formation of a structurally frozen hydration layer for a particle diffusing in water and is responsible for a substantial speedup of translational diffusion compared to traditional theories of dielectric friction. Diffusion of proteins is insensitive to charge mutations, while smaller particles with asymmetric charge distribution can show a strong dependence of translational and rotational diffusion on molecular charge. Dielectric calculations of the electrostatic force require low vales $\simeq 5$ for the effective dielectric constant of interfacial water to be consistent with simulations.

TOC Graphic

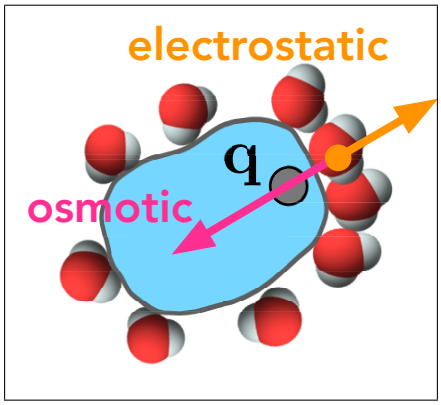

In his followup paper on Brownian motion published in 1908,[1] Einstein noted that the physical driving force of macroscopic diffusion is the microscopic osmotic pressure. It arises from a lower chemical potential of the solvent on the side of a diffusing particle facing higher concentration of solutes. Molecules of the solvents rushing toward lower chemical potential produce a gradient of the solvent density, which in turn leads to osmotic pressure pushing the particle down the concentration gradient. This argument equally applies to a single Brownian particle for which compression and decompression density fluctuations caused by thermal agitation on different sides of a tagged particle are responsible for random forces of Brownian motion.

The notion of osmotic pressure driving diffusivity and Brownian motion can be extended to polarization of the interface by ionic charges. An asymmetric charge distribution, such as the off-center charge shown in Figure 1, will both compress a polar liquid on one side of the particle and polarize the interface thus shifting the chemical potential:[2] $\mu(E) = \mu(0) - (E^2/8\pi)(\partial\epsilon/\partial\rho)_T$. An inhomogeneous electric (Maxwell) field E will alter the local dielectric constant ϵ because of its dependence on the local density as expressed by the isothermal density derivative $(\partial\epsilon/\partial\rho)_T$. An inhomogeneous chemical potential at the interface of a Brownian particle translates to differences in local pressure[3] and, correspondingly, to an osmotic force induced by polarizing the medium.

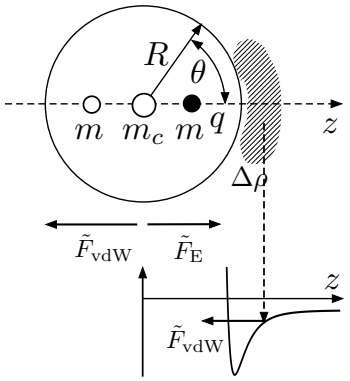

Figure 1: Schematic representation of the solute with the off-center charge q. The lower portion shows the van der Waals (vdW) interaction potential and the vdW force acting from the density augmentation $\Delta\rho$ caused by electrostatics. The vdW force $\tilde{F}_{\rm vdW}$ is directed opposite to the electrostatic force $\tilde{F}_E$. Forces with tildes refer to the body frame of reference. The solute is constructed with three sites with off-center masses m and the center mass m_c. One of the off-center sites carries the charge q. The effective radius of the solute R is calculated from eq 15.

From the molecular perspective, a density enhancement $\Delta\rho$ on one side of a tagged particle implies imbalance of the van der Waals (vdW) interaction between the particle and surrounding liquid. The osmotic pressure of Einstein's argument becomes the vdW force $\tilde{F}_{\rm vdW}$ in Figure 1 acting in the direction opposite to the side of the density increment (see the bottom part of the figure for a qualitative argument). At equilibrium, one anticipates that the vdW force is compensated by the electrostatic force $\tilde{F}_E$ between the charge q and the liquid polarized by it. This is the situation that we report here for a number of protein mutants studied by molecular dynamics (MD) simulations in an aqueous solution. Once the hydration shell has sufficient room for the density gradient to establish, a full compensation between electrostatic and vdW forces is realized.[4] However, for small solutes, the osmotic push to increase the local density encounters frustration due to repulsive molecular cores and other intermolecular interactions between the water molecules in the hydration shell. A full compensation might not be realized. We find this scenario for a small solute with the off-center charge shown in Figure 1. The vdW force turns out to exceed the electrostatic force (Figure 2a) and we find for the z-projections of the forces in the body frame of the solute (denoted with tildes)

$$\langle \tilde{F}_z \rangle = \langle \tilde{F}_{\rm vdw} \rangle + \langle \tilde{F}_E \rangle < 0 \tag{1}$$

Of course, the net force on the solute is zero in the laboratory frame. The body-frame projection $\langle \tilde{F}_z \rangle$ is averaged out by solute's rotations and $\langle F_z \rangle = 0$ in the laboratory frame (denoted without tilde).

A strong electrostatic pull from the solute charges creates a new physical reality of a strongly structured hydration shell, which tends to rotate together with the solute. (We stress that it is the arrested structure that moves with the solute, the water molecules can still exchange with the bulk.[5,6]) If this mechanism is fully realized, fluctuations of both vdW and electrostatic forces can be identified with the unit vector $\hat{\mathbf{u}}$ along the axis of rotation in the solute body frame

$$\delta\mathbf{F}_{\rm vdW} = \langle \tilde{F}_{\rm vdw} \rangle \hat{\mathbf{u}}, \quad \delta\mathbf{F}_E = \langle \tilde{F}_E \rangle \hat{\mathbf{u}} \tag{2}$$

The variance of the total force $\mathbf{F} = \mathbf{F}_{\rm vdW} + \mathbf{F}_E$ in the laboratory frame includes a negative cross-correlation $\langle \delta\mathbf{F}_{\rm vdW} \cdot \delta\mathbf{F}_E \rangle$. If $\langle \tilde{F}_z \rangle = 0$ in eq 1, $\langle \delta\mathbf{F}_{\rm vdW} \cdot \delta\mathbf{F}_E \rangle = -\langle (\delta\mathbf{F}_E)^2 \rangle$ and the force variance comes as a result of subtraction between self vdW and electrostatic terms[4,5,7]

$$\langle (\delta\mathbf{F})^2 \rangle = \langle (\delta\mathbf{F}_{\rm vdW})^2 \rangle - \langle (\delta\mathbf{F}_E)^2 \rangle \tag{3}$$

Equation 3 is highly nontrivial. It is accurate for solvated proteins[4] and dipolar solutes,[5,8] but is not exactly followed for small ions[9] and spherical solutes studied here and for charged nanoparticles studied elsewhere.[7] The reason is an incomplete compensation between the vdW and electrostatic forces, leading to a negative total force in the body frame in eq 1.

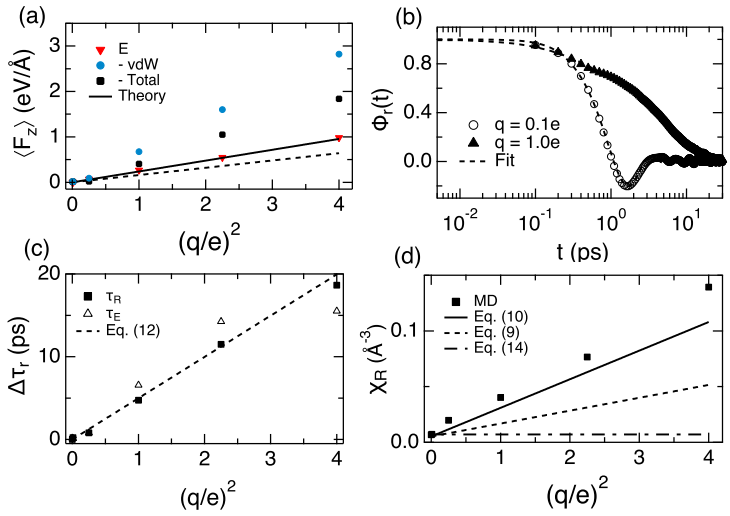

Figure 2: (a) Components of the average force acting on the spherical solutes. The lines show calculations with eqs 9 (dashed) and 10 (solid). Negative values of the vdW and total average forces are shown in the plot. (b) Rotational correlation function $\Phi_r(t)$ at $q = 0.1$ (circles) and $q = 1.0$ (triangles). The dashed lines are fits to analytical equations discussed in the SI. (c) Increment of the rotational time $\Delta\tau_r = \tau_r - \tau_r^0$ and the relaxation time of the electric field τ_E. The dashed line shows the calculation according to eq 12. (d) Reaction-field susceptibility $\chi_R = (\beta/6)\langle (\delta\mathbf{E}_s)^2 \rangle$ from MD (points) compared with eq 13 in which $\langle \tilde{F}_E \rangle$ is either from eq 10 (solid line) or from eq 9 (dashed line). The dash-dotted horizontal line refers to the continuum linear response from eq 14; all calculations are done with $R = 4.1$ Å (eq 15) and $\epsilon = \epsilon_{\rm int} = 5$.

The variance of the force acting on the particle directly affects friction imposed by the solvent on the diffusing particles. The memory equation specifying the velocity correlation function through the memory kernel[10] connects the friction coefficient ζ to the force variance and the integrated

memory time τ_m

$$\zeta = (\beta/3)\langle(\delta\mathbf{F})^2\rangle\tau_m \tag{4}$$

Therefore, reduction of the breadth of force fluctuations through electrostatic forces according to eq 3 reduces the friction experienced by the diffusing particle. This scenario, if realized, should enhance the translational diffusion coefficient $D_t = (\beta\zeta)^{-1}$, $\beta = (k_{\mathrm{B}}T)^{-1}$. The result is opposite to the commonly anticipated slowing down of translational diffusion by electrostatic interactions of an ion with the polar liquid known as dielectric friction. The vdW and electrostatic forces are viewed as uncorrelated in traditional theories,[11–15] leading to additivity of the vdW and electrostatic friction components $\zeta = \zeta_{\mathrm{vdW}} + \zeta_E$, where the electrostatic component ζ_E becomes[9]

$$\zeta_E = \frac{\beta q^2}{3}\tau_E\langle(\delta\mathbf{E}_s)^2\rangle \tag{5}$$

In eq 5, the electrostatic force $\mathbf{F}_E = q\mathbf{E}_s$ is given in terms of the electric field of the solvent $\mathbf{E}_s$ acting on charge q. Further, the memory time is replaced with the field relaxation time τ_E; $\delta\mathbf{E}_s = \mathbf{E}_s - \langle\mathbf{E}_s\rangle$. Correspondingly, D_t^{-1} is predicted[9,14] to scale linearly with the squared ionic charge q^2 reflecting slower diffusion for solutes carrying higher charges. The new mechanism of diffusivity enhancement discussed here predicts just an opposite effect of the solute-solvent electrostatic interaction: in contrast to diffusivity reduction in the standard formulation, a strong negative cross-correlation between vdW and electrostatic forces (eq 3) enhances particle's diffusivity.

The electrostatic force acting on the particle along the z-axis in the body frame is obtained by surface integration of the Maxwell stress tensor $T_{z\beta}$, contracted with the Cartesian components $\hat{n}_\beta$ of the outward unit vector normal to the surface[2,3,16]

$$\langle\tilde{F}_E\rangle = \oint T_{z\beta}\hat{n}_\beta dS \tag{6}$$

where dS is the surface area differential and summation runs over the common Cartesian indexes

β. The Maxwell stress tensor[2]

$$T_{\alpha\beta} = \sigma_{\alpha\beta} + \frac{1}{8\pi}\delta_{\alpha\beta}E^2\rho\left(\frac{\partial\epsilon}{\partial\rho}\right)_T \tag{7}$$

is defined in terms of Cartesian components of the electric field E_α and is a sum of

$$\sigma_{\alpha\beta} = (4\pi)^{-1}\epsilon\left(E_\alpha E_\beta - \tfrac{1}{2}\delta_{\alpha\beta}E^2\right) \tag{8}$$

and the compression component $\propto \rho(\partial\epsilon/\partial\rho)_T$.

The force arising from $\sigma_{\alpha\beta}$ integrates to zero over the surface of the spherical solute (see Supporting Information (SI) for a derivation). On the contrary, the compression term yields

$$\langle\tilde{F}_E\rangle = \frac{q^2}{R^2}\rho\left(\frac{\partial\epsilon}{\partial\rho}\right)_T\sum_{\ell=0}^{\infty}\left(\frac{s}{R}\right)^{2\ell+1} (\ell+1)A_{\ell+1}\left[A_\ell + A_{\ell+2}\left(\frac{s}{R}\right)^2\right] \tag{9}$$

where s is the distance to the charge from the center of a spherical solute with the radius R (Figure 1) and $A_\ell = (\ell+1)/[\ell(\epsilon+1)+\epsilon]$. The physical reason for this result is clear: the energy of the dipoles is lower in the stronger field and the liquid dipoles are drawn to the region with a higher field as long as liquid's compressibility permits a density contraction.

Alignment of molecular dipoles to the external field and liquid's compression in the nearest vicinity of the solute do not have to follow the predictions of the dielectric theory. In addition, the derivation of eq 9 assumes that both the normal and tangential components of the Maxwell stress are allowed at the solute surface. The tangential stress might not be sustained by the interfacial liquid, which will flow instead.[3] Dropping the tangential component of the stress leads to

$$\langle\tilde{F}_E\rangle = \frac{q^2}{R^2}\left[\epsilon + \rho\left(\frac{\partial\epsilon}{\partial\rho}\right)_T\right]\sum_{\ell=0}^{\infty}(\ell+1)A_\ell A_{\ell+2}\left(\frac{s}{R}\right)^{2\ell+1} \tag{10}$$

which makes $\langle\tilde{F}_E\rangle$ about 50% higher (see SI). These alternative scenarios are tested against mi-

croscopic numerical simulations presented below. We find that eq 10 provides a better description of the simulation results. For the sake of an estimate, the Kirkwood-Onsager equation[17] for the dielectric constant of a polar liquid suggests that $\rho(\partial\epsilon/\partial\rho)_T \simeq \epsilon$ (neglecting the density dependence of the Kirkwood factor). One indeed finds $\rho(\partial\epsilon/\partial\rho)_T \simeq 81$ for water at $T \simeq 300$ K when $\epsilon \simeq 78$.[17] Correspondingly, one obtains[18] $\rho(\partial\epsilon/\partial\rho)_T \simeq 83$ with $\epsilon \simeq 73$ for SPC/E water used in our MD simulations. From this estimate, eq 9 predicts $\langle \tilde{F}_E \rangle \simeq 38$ pN acting on the solute with the radius $R = 3$ Å similar to the one used in our simulations.

MD simulations of solutes carrying six different charges q ranging from $q = 0.01e$ to $q = 2.0e$ (e is the elementary charge) in SPC/E water have been conducted as detailed in the SI. In addition, we have performed simulation of forces acting on six charge mutants of the protein azurin carrying charges from $q = 0$ to $q = -5e$. The protein simulations follow the protocol described elsewhere.[4]

The buildup of a structurally frozen hydration shell with increasing solute charge is reflected by changes in the character of rotational dynamics. The rotational correlation function $\Phi_r(t) = \langle \hat{\mathbf{u}}(t) \cdot \hat{\mathbf{u}}(0) \rangle$ qualitatively changes its behavior from inertial dynamics (with oscillations) at low charge values to a smoothly decaying function, which is well fitted by two decaying exponents, at higher values of q (Figure 2b, see SI). The dynamics are thus inertial at small electrostatic interactions and become overdamped with increasing electrostatic pull.

Rotational diffusion is affected by electrostatics through the delayed response of the liquid dipoles to rotations of the solute dipole sq. This dielectric friction mechanism increases the rotational relaxation time[19] from the value τ_r^0 in the absence of electrostatic interactions to the value

$$\tau_r = \tau_r^0 + \frac{(\beta sq)^2}{6} \tau_E \langle (\delta \mathbf{E}_s)^2 \rangle \tag{11}$$

Dielectric theories for the field relaxation time τ_E and for the variance of electrostatic fluctuations produce the following estimate[5]

$$\tau_r^c = \tau_r^0 + \frac{3\beta(sq)^2}{R^3} \frac{\epsilon - 1}{(2\epsilon + 1)^2} \tau_D \tag{12}$$

where τ_D is the Debye relaxation time of the solvent ($\tau_D \simeq 10.4$ ps for SPC/E water[9]). The straight line in Figure 2c compares MD simulations for $\Delta\tau_r = \tau_r - \tau_r^0$ to eq 12. Overall, altering the solute charge from $q = 0$ to $q = 2$ leads to a retardation factor of $\sim 10^2$ for the rotational dynamics. Similar extent of rotational retardation, by a factor of $\simeq 183$, was previously found[5] for a dipolar diatomic in SPC/E water when its dipole moment was raised to $\simeq 15$ D.

The variance of the electrostatic force $\langle(\delta\mathbf{F}_E)^2\rangle = q^2\langle(\delta\mathbf{E}_s)^2\rangle$ is expected to scale linearly with q^2 in linear response theories such that the variance of the electrostatic field of the solvent is independent of the solute charge (no perturbation of the solvent structure). In contrast, we find a linear scaling of the field variance with q^2 (Figure 2d). It arises from rotations of the average molecular-frame field $\langle\tilde{F}_E\rangle/q$ producing an overall non-Gaussian distribution of the field in the laboratory frame.[5] Solute rotations add an additional term to the field variance equal to $(\langle\tilde{F}_E\rangle/q)^2$. According to eqs 9 and 10, the electrostatic force $\tilde{F}_E$ scales linearly with q^2 and an additional term in the force variance should scale as $\propto q^4$. This expectation can be viewed in terms of the reaction field susceptibility[9] $\chi_R = (\beta/6)\langle(\delta\mathbf{E}_s)^2\rangle$ as follows

$$\chi_R = \chi_R^L + (\beta/6)(\langle\tilde{F}_E\rangle/q)^2 \tag{13}$$

where continuum approximation can be adopted for the linear-response reaction field susceptibility[17,20] χ_R^L

$$\chi_R^L = \frac{1}{R^3}\frac{\epsilon - 1}{2\epsilon + 1} \tag{14}$$

According to eq 13, χ_R should be a linear function of q^2. Equations 13 and 14 reproduce the MD result (Figure 2d) when the effective solute radius $R \simeq 4.1$ Å is calculated from the solute-solvent radial distribution function $g_{0s}(r)$ according to the relation[9]

$$R^{-3} = 3\int_0^\infty (dr/r^4) g_{0s}(r) \tag{15}$$

A number of recent simulation[6,21,22] and experimental[23] studies have shown that a significant

reduction of the dielectric constant is required to characterize polarization of water in the interface. We find that recovering the values of the average electrostatic force $\langle \tilde{F}_E \rangle$ (eq 10) in Figure 2a and of χ_R (eq 13) in Figure 2d requires an effective dielectric constant of the interface $\epsilon_{\text{int}} \simeq 5$, which is in agreement with simulations of water interfacing a spherical solute.[22] Simulation of interfacial water have also shown that the dielectric constant is highly anisotropic in the interface, with a low dielectric constant in the direction perpendicular to the dividing surface and the tangential projection being bulk-like or exceeding bulk water in polarity.[24,25] Since the force in eqs 9 and 10 drops as ϵ^{-1}, the tangential component of the force is of lesser significance even if water does not slip on the solute surface. This observation lends additional support to eq 10, which suppresses the tangential force component, over eq 9 allowing it.

Estimating the density derivative of the interface dielectric constant is currently not feasible and the results shown in Figure 2 are obtained by assuming $\rho \left(\partial \epsilon_{\text{int}}/\partial \rho\right)_T \simeq \epsilon_{\text{int}}$ in analogy with similar relations found for bulk laboratory and SPC/E water. We additionally find that the dynamics of the electric field follow the rotational dynamics of the solute. The exponential relaxation time τ_E of the time correlation function $C_E(t) = \langle \delta \mathbf{E}_s(t) \cdot \delta \mathbf{E}_s(0) \rangle$ mostly matches the rotational relaxation time τ_r (Figure 2c). Similarly to the electrostatic forces, we find that the variance of the vdW force divided with q^2, $\langle (\delta F_{\text{vdW}})^2 \rangle / q^2$, is a linear function of q^2 (see SI). The reason for this phenomenology also lies in rotations of the solute producing a term in the force variance equal to $\langle \tilde{F}_{\text{vdW}} \rangle^2$. Since this average force scales as $\propto q^2$ (Figure 2a), the corresponding contribution to the variance scales as $\propto q^4$.

The distributions of component forces ($a = \text{E, vdW}$) projected on the axis of symmetry for the spherical solute and azurin are shown in Figure 3a,b. For azurin mutants, the direction of the electrostatic force in the body frame of the protein is chosen as the symmetry axis in analogy with the spherical solute (Figure 1). In all cases studied here, the distribution of the vdW force is broader, as required to produce the overall positive variance in eq 3. As mentioned above, the main distinction between the spherical solute and protein mutants is that the total force has a nonzero average value for the former and averages to zero for the proteins. The nonzero average force produces an

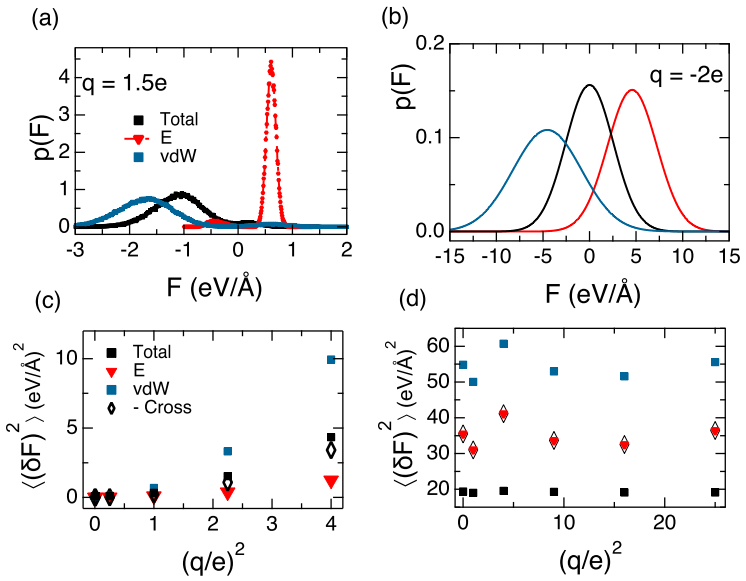

Figure 3: Distributions of electrostatic (E), vdW, and total force projected on the symmetry axis of the spherical solute with $q = 1.5e$ (a) and azurin protein carrying the charge $q = -2e$ (oxidized state, b). Electrostatic and vdW self components of the force variance and the negative of the cross correlation, $-\langle \delta\mathbf{F}_{\rm vdW} \cdot \delta\mathbf{F}_E \rangle$, are shown for the spherical solutes (c) and protein mutants (d).

additional component in the variance related to solute rotations and we find the following relation between the laboratory-frame and body-frame variances to hold for either force components or for the total force

$$\langle (\delta F_a)^2 \rangle = \langle \tilde{F}_a \rangle^2 + \langle (\delta \tilde{F}_a)^2 \rangle \tag{16}$$

Changes of the component variances and the total force variance with the solute charge are also distinct for proteins and spherical solutes. The variances are essentially independent of the protein charge and show an exact compensation between the self electrostatic and cross electrostatic-vdW terms according to eq 3 (Figure 3d). In contrast, there is a substantial dependence of variance components on q for the spherical solutes. Moreover, the cross term overshoots the electrostatic variance in the latter case, thus further reducing the total force variance compared to the naive additivity assumption. In all these cases, the variance of the force is substantially reduced compared to the additivity assumption of the Born picture[11] adopted in the traditional theories of dielectric friction.[11–14] According to the general result of eq 4, such a compensatory mechanism must reduce the friction experienced by the solute and enhance its diffusivity. An indication of difficulties of

traditional theories of dielectric friction comes from experimental studies of rotational dynamics of optical chromophores when one anticipates[26] $\Delta\tau_r = \tau_r - \tau_r^0$ (eq 11) to scale with the Stokes shift ΔE^{St} as $\Delta\tau_r \propto \Delta E^{\mathrm{St}}\tau_E$. The expected proportionality has indeed been observed experimentally,[27,28] but the slope of this correlation was found to be grossly inconsistent with theoretical expectations.

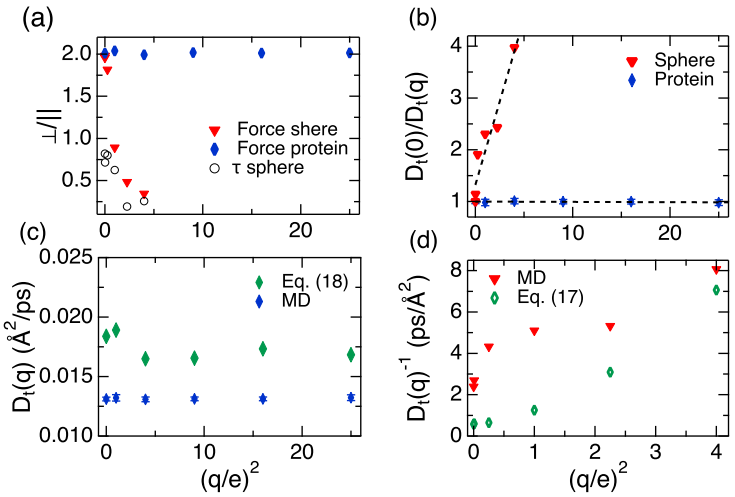

Figure 4: (a) Ratio $\langle(\delta\tilde{F}_\perp)^2\rangle/\langle(\delta\tilde{F}_\parallel)^2\rangle$ for the protein mutants and spherical solutes (filled points) and $\tau_F^\perp/\tau_F^\parallel$ for spherical solutes (open points). (b) Translational diffusion coefficient $D_t(0)/D_t(q)$ for spherical solutes and protein mutants. The dashed lines are linear regressions. (c) Diffusion coefficients of protein mutants from MD compared with eq 18. The error bars in MD values are estimated from multiple short trajectories.[4] (d) Diffusion coefficients of spherical solutes from MD compared to eq 17.

Given that rotations of the average force $\langle\tilde{F}_z\rangle$ do not contribute to translational diffusion, only force fluctuations in the body frame need to be considered. The translational diffusion coefficient becomes

$$D_t^{-1} = (\beta^2/3)\sum_{\alpha=\parallel,\perp}\langle(\delta\tilde{F}_\alpha)^2\rangle\tau_m^\alpha \tag{17}$$

where τ_m^α are integral memory times for the parallel ($\parallel$) and perpendicular ($\perp$) force projections. The asymmetry of the force fluctuations enhances with increasing q for spherical solutes such a that the ratio $\langle(\delta\tilde{F}_\perp)^2\rangle/\langle(\delta\tilde{F}_\parallel)^2\rangle$ deviates down from the value of 2 of the isotropic limit (Figure 4a). This does not happen for the protein mutants which maintain isotropic force fluctuations in

the body frame. Assuming the memory times to be close in magnitude to the force relaxation time τ_F, a simplified equation can be written

$$D_t^{-1} \simeq (\beta^2/3)\langle(\delta\tilde{F})^2\rangle\tau_F \tag{18}$$

It predicts little effect of charge on the diffusion constant for proteins since both the force relaxation time and the force variance are insensitive to q. This expectation is in accord with empirical evidence.[29] The diffusion coefficients shown in Figure 4b,c were calculated from simulations[4] as described in the SI including corrections[30] for the finite size of the simulation box. Equation 18 is found to overestimate the MD values by ~ 8 % (Figure 4c).

Altering force variances, their asymmetry, and shortening force relaxation times all contribute to a strong dependence of the translational diffusion coefficient of the spherical solutes on q. The ratio $D_t(0)/D_t(q)$ scales roughy linearly with q^2 (Figure 4b). When $\tau_m^\alpha \simeq \tau_F^\alpha$ is used in eq 17, this approximation does not reproduce MD results at small values of q, but the agreement is much improved when q is increased (Figure 4d). The memory time τ_m (eq 4) significantly exceeds τ_F for a loose hydration shell of a weakly charged solute, but it shortens with shell tightening to converge to the memory-free limit of the standard Langevin equation. Linear scaling of D_t^{-1} with q^2 is qualitatively in line with the predictions of dielectric friction theories (eq 5), although a quantitative agreement cannot be reached because of significant cross-correlations between vdW and electrostatic forces observed here (Figure 3c). The strong effect of charge on the diffusion constant for the spherical solutes is consistent with previous simulations for charges placed at the solute center,[9] where an increase of D_t^{-1} by a factor of $\simeq 3.7$ was found per single charge added to the solute.

In conclusion, strong electrostatic pull of charges close to the water interface leads to an emergence of a structurally frozen hydration shell. This new physical reality requires a new description of mobility, which, due to its specific physical nature, also allows some simplifications and general predictions. The main novel result of this physics is a strong compensation between cross-correlations of electrostatic and vdW forces and their self variances. This destructive interference

leads to a decrease of the effective breadth of the force fluctuations responsible for random kicks on a tagged particle. The insuring reduction of friction leads to a higher diffusivity.

One has to stress that the effects discussed here and the corresponding corrections to the traditional theories of dielectric friction are very substantial. When the relaxation times τ_E and field variances $\langle(\delta\mathbf{E}_s)^2\rangle$ specific for proteins are used in eq 11, one obtains $\zeta_E/\zeta_{\text{vdW}} \simeq 10^6$ for proteins carrying a nonzero charge, where ζ_{vdW} is the Stokes-Einstein friction. The standard theories thus prohibit protein diffusion in water. This dramatic failure is remedied by strong correlations between electrostatic and vdW forces allowed by the structured hydration layer of a protein in solution. Tweaking the destructive interference in eq 3 by an enzymatic reaction can potentially enhance protein diffusion.[31] Specifically, a chemical reaction instantaneously altering the protein charge distribution is expected to destroy the balance between electrostatic and vdW forces leading to a transient nonzero force $\langle\tilde{F}_E\rangle_t$ similar to the one observed here for the off-center solutes (Figure 2a). If the equilibration time for $\langle\tilde{F}_E\rangle_t \to 0$ is sufficiently long, one can potentially observe jerks in protein displacements.

Common to all diffusion phenomena is the gradient of the osmotic pressure[1] establishing equilibrium between surface vdW forces caused by density augmentation and electrostatic forces caused by asymmetric charge distribution (Figure 1). The electrostatic force, $\langle\tilde{F}_E\rangle \propto q^2 s/(\epsilon R^3)$, decays with increasing solute size and the effect of electrostatics should diminish for larger colloidal particles. This drop in significance of electrostatics is partially offset by a low effective dielectric constant ϵ_{int} of water in the hydration layer[6,21–23,32] quantified by replacing $\epsilon \to \epsilon_{\text{int}}$ in eqs 9 and 10. For colloidal particles with distributed surface charge, such as proteins, equations for the electric force presented here (eqs 9 and 10) need to be extended to account for multiple charges q_i with positions s_i positioned close to the interface.

Supporting Information Available

Simulation protocol, derivation of equations for the electrostatic force, and the analysis of MD

simulations.

Notes

The authors declare no competing financial interests.

Acknowledgement

This research was supported by the National Science Foundation (CHE-1800243) and through XSEDE resources (TG-MCB080071) as well as ASU's Research Computing for computational resources.

References

(1) A. Einstein, Z. Electrochem. 14, 235 (1908), In *Investigations on the Theory of the Brownian Movement*; Furth, R., Ed.; BN Publishing, 2011.

(2) Landau, L. D.; Lifshitz, E. M. *Electrodynamics of Continuous Media*; Pergamon: Oxford, 1984.

(3) Stratton, J. A. *Electromagnetic Theory*; McGraw-Hill Inc.: New York, 1941.

(4) Sarhangi, S. M.; Matyushov, D. V. Driving forces of protein diffusivity. *J. Phys. Chem. Lett.* **2020**, *11*, 10137–10143.

(5) Samanta, T.; Matyushov, D. V. Dielectric friction, violation of the Stokes-Einstein-Debye relation, and non-Gaussian transport dynamics of dipolar solutes in water. *Phys. Rev. Res.* **2021**, *3*, 023025.

(6) Mondal, S.; Bagchi, B. Water layer at hydrophobic surface: Electrically dead but dynamically alive? *Nano Lett.* **2020**, *20*, 8959–8964.

(7) Cui, A. Y.; Cui, Q. Modulation of nanoparticle diffusion by surface ligand length and charge: Analysis with molecular dynamics simulations. *J. Phys. Chem. B* **2021**, *125*, 4555–4565.

(8) Kumar, P. V.; Maroncelli, M. The non-separability of "dielectric" and "mechanical" friction in molecular systems: A simulation study. *J. Chem. Phys.* **2000**, *112*, 5370–5381.

(9) Samanta, T.; Matyushov, D. V. Mobility of large ions in water. *J. Chem. Phys.* **2020**, *153*, 044503.

(10) Balucani, U.; Zoppi, M. *Dynamics of the Liquid Phase*; Clarendon Press: Oxford, 1994.

(11) Born, M. Uber die Beweglichkeit det elektrolytischen Ionen. *Z. Phys.* **1920**, *1*, 221–249.

(12) Zwanzig, R. Time-correlation functions and transport coefficients in statistical mechanics. *Ann. Rev. Phys. Chem.* **1965**, *16*, 67–102.

(13) Wolynes, P. Dynamics of electrolyte solutions. *Ann. Rev. Phys. Chem.* **1980**, *31*, 345–376.

(14) Bagchi, B. *Molecular Relaxation in Liquids*; Oxford University Press: Oxford, 2012.

(15) Banerjee, P.; Bagchi, B. Ions' motion in water. *J. Chem. Phys.* **2019**, *150*, 190901.

(16) Jackson, J. D. *Classical Electrodynamics*; Wiley: New York, 1999.

(17) Matyushov, D. V. *Manual for Theoretical Chemistry*; World Scientific Publishing Co. Pte. Ltd.: New Jersey, 2021.

(18) Teplukhin, A. V. Thermodynamic and structural characteristics of SPC/E water at 290 K and under high pressure. *J. Struct. Chem.* **2019**, *60*, 1590–1598.

(19) Nee, T. W.; R. Zwanzig, R. Theory of dielectric relaxation in polar liquids. *J. Chem. Phys.* **1970**, *52*, 6353–6363.

(20) Onsager, L. Electric moments of molecules in liquids. *J. Am. Chem. Soc.* **1936**, *58*, 1486–1493.

(21) Bonthuis, D. J.; Gekle, S.; Netz, R. R. Dielectric profile of interfacial water and its effect on double-layer capacitance. *Phys. Rev. Lett.* **2011**, *107*, 166102.

(22) Dinpajooh, M.; Matyushov, D. V. Dielectric constant of water in the interface. *J. Chem. Phys.* **2016**, *145*, 014504.

(23) Fumagalli, L.; Esfandiar, A.; Fabregas, R.; Hu, S.; Ares, P.; Janardanan, A.; Yang, Q.; Radha, B.; Taniguchi, T.; Watanabe, K. et al. Anomalously low dielectric constant of confined water. *Science* **2018**, *360*, 1339–1342.

(24) Loche, P.; Ayaz, C.; Wolde-Kidan, A.; Schlaich, A.; Netz, R. R. Universal and nonuniversal aspects of electrostatics in aqueous nanoconfinement. *J. Phys. Chem. B* **2020**, *124*, 4365–4371.

(25) Motevaselian, M. H.; Aluru, N. R. Confinement-induced enhancement of parallel dielectric permittivity: Super permittivity under extreme confinement. *J. Phys. Chem. Lett.* **2020**, *11*, 10532–10537.

(26) van der Zwan, G.; Hynes, J. T. Time-dependent fluorescence solvent shifts, dielectric friction, and nonequilibrium solvation in polar solvents. *J. Phys. Chem.* **1985**, *89*, 4181.

(27) Horng, M. L.; Gardecki, J. A.; Papazyan, A.; Maroncelli, M. Subpicosecond measurements of polar solvation dynamics: Coumarin-153 revisited. *J. Phys. Chem.* **1995**, *99*, 17311–17337.

(28) Gayathri, B. R.; Mannekutla, J. R.; Inamdar, S. R. Rotational diffusion of coumarins in alcohols: a dielectric friction study. *J. Fluoresc.* **2008**, *18*, 943–952.

(29) Young, M. E.; Carroad, P. A.; Bell, R. L. Estimation of diffusion coefficients of proteins. *Biotech. Bioeng.* **1980**, *22*, 947–955.

(30) Yeh, I. C.; Hummer, G. System-size dependence of diffusion coefficients and viscosities from molecular dynamics simulations with periodic boundary conditions. *J. Phys. Chem. B* **2004**, *108*, 15873–15879.

(31) Jee, A.-Y.; Cho, Y.-K.; Granick, S.; Tlusty, T. Catalytic enzymes are active matter. *Proc. Natl. Acad. Sci. USA* **2018**, *115*, E10812.

(32) Seyedi, S.; Matyushov, D. V. Dipolar susceptibility of protein hydration shells. *Chem. Phys. Lett.* **2018**, *713*, 210–214.